Available online at www.sciencedirect.com
SCIENCE DIRECT
Carbohydrate Research 341 (2006) 1029–1040
Carbohydrate RESEARCH

A theoretical study of glucose mutarotation in aqueous solution

Alexander M. Silva,[a] Edilson C. da Silva[b] and Clarissa O. da Silva[a,*]

[a]*Departamento de Química, Universidade Federal Rural do Rio de Janeiro, BR 465 km 7, Seropédica, RJ 23890-000, Brazil*
[b]*Departamento de Fisico-Química, Instituto de Química, Universidade Federal do Rio de Janeiro, Cidade Universitária, CT Bloco A, Rio de Janeiro, RJ 21949-900, Brazil*

Received 5 July 2005; accepted 16 February 2006
Available online 11 April 2006

Abstract—In this work the mechanism of glucose mutarotation is investigated in aqueous solution considering the most likely pathways proposed from experimental work. Two mechanisms are studied. The first involves an intramolecular proton transfer as proposed by textbooks of organic chemistry, and the second uses one solvent water molecule to assist proton transfer. Both mechanisms are studied in the gas phase and in aqueous solution with the help of a polarizable continuum model, which is adopted to introduce the electrostatic nonspecific influence of bulk solvent. The structures are fully characterized through the calculation of the corresponding vibrational frequencies. The rate coefficients for each mechanism are calculated following transition-state theory in both the gas phase and in aqueous solution. Values computed for the water-assisted pathway in the continuum solvent agree best with the experimental results.

Keywords: Glucose mutarotation; Rate coefficients; Glucose reaction

1. Introduction

Aldoses and ketoses are classes of organic compounds that play very important biological roles.[1] Their mutarotation reaction has been studied extensively.[2] Through the generation of a hemiacetal, this reaction is responsible for the interconversion between their cyclic forms that differ in configuration at the anomeric carbon and the acyclic forms as shown in Figure 1. Although the acyclic form of glucose occurs, more than 99% of the glucose in aqueous solution is in the pyranosidic form.[3]

Brønsted and Guggenheim[4] reported the first kinetic study of this reaction. They proposed that the mutarotation of glucose may follow either acid or base catalysis. So far, several mechanistic proposals have been reported. The first is due to Lowry[5] who proposed a trimolecular reaction involving the substrate, an acid and a base. Later, Swain and collaborators[6] showed that

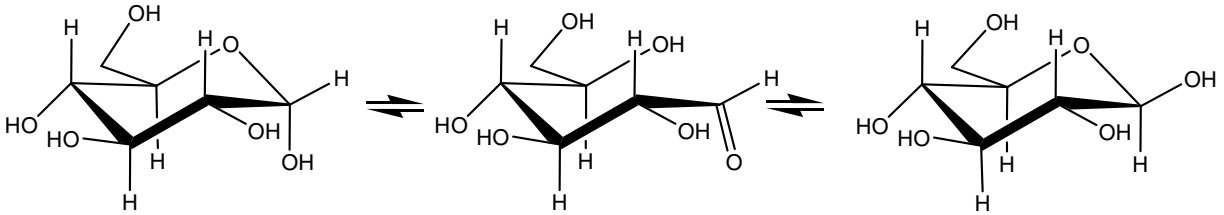

Figure 1. Mutarotation of glucose.

* Corresponding author. Tel./fax: +55 21 26822807; e-mail: clarissa-dq@ufrrj.br

0008-6215/$ - see front matter © 2006 Elsevier Ltd. All rights reserved.
doi:10.1016/j.carres.2006.02.035

Lowry's proposal was inconsistent with the available experimental data. Pedersen reported a reaction mechanism[7] that proceeds via two bimolecular steps. The first step was catalyzed by acid through protonation of the ring oxygen, and the second concerted step involved the removal of the hydroxyl group and simultaneous breakage of the ether linkage. This resulted in the formation of the free aldehyde form and was the rate-determining step. This mechanism is also in disagreement with experimental results.[8]

Nowadays, the most accepted mechanism involves the formation of the free aldehyde form (confirmed by polarography studies[9]), resulting in a pseudo first-order reaction for the substrate.

The conversion of the pyranoses to the aldehyde form of glucose follows three stages, following the labeling adopted for carbohydrates: (1) the protonation of the O5, (2) the breaking of the O1–H bond (intramolecular transfer), and (3) the breaking of the O5–C1 bond. This mechanism has a stepwise (1) and a concerted (2 and 3) step. However, if we assume that these three processes take place in a stepwise way, such a mechanism does not agree with the available experimental data. The mechanism proposed by Pedersen is an example of a stepwise mechanism that shows a disagreement with experimental data.[7] Eigen suggested a different concerted mechanism. The main characteristic of his proposal is that the two proton transfers could proceed in aqueous solution via a pathway involving two or more water molecules in a cyclic hydrogen-bonded transition state,[10] where the intramolecular proton transfer does not take place in aqueous solution. There is some experimental evidence for the solvent participation in the mutarotation reaction that appears from the studies of primary solvent effects on the rates of glucose and tetramethylglucose observed in $H_2O + D_2O$ mixtures.[11] Besides that, the absence of intramolecular proton transfer can be inferred from the small values found for the mutarotation rate of glucose in organic solvents[12] and other factors.[13] The previous work has shown that the reaction order with respect to water is zero for an acid-catalyzed reaction involving a stepwise mechanism, which is in agreement with Pedersen's proposal. But when the system is in aqueous solution, the conclusions are less reliable. They suggest that about three water molecules may be involved, and this solvent-catalyzed process may involve a concerted mechanism.

Rittenberg and Graff[14] have observed that the ^{18}O1 atom of glucose undergoes oxygen exchange with water approximately 30 times more slowly than the mutarotation reaction. This excludes pathways that do not proceed via ring opening, such as one that involves exchange of the hydroxyl group at C1 with the hydroxyl group of water. Furthermore, the free aldehyde mechanism is consistent with Brønsted and Guggenheim's kinetic study mentioned above.

Although the vapor pressure of carbohydrates is very low at room temperature, and the amount in the gas phase is negligible, the mutarotation is always explained in specialized textbooks of organic chemistry as a general intramolecular process and no solvent is considered. Because mutarotation is observed mainly in solution, the solvent cannot be disregarded.

Yamabe and Ishikawa[15] have performed a theoretical quantum mechanics study of the mutarotation of glucose in aqueous solution using the Onsager model,[16] assisted by a few water molecules. They concluded that two or three water molecules may assist this reaction through a 'strain-free hydrogen-bond network' for ready proton transfer. The reaction barrier for the pyranose ring opening is strongly reduced by this water assistance: the barrier height goes from 50.84 kcal/mol in an intramolecular proton transfer to 24.88 kcal/mol, where the reaction is assisted by three water molecules. However, in their work, these authors used only the trans gauche (TG) conformers of α- and β-D-glucose. This is not the most abundant conformer of glucose in aqueous solution.[17] Besides that, there are some important considerations with regard to the reference structures used in each cluster investigated by these authors that will be properly addressed in the next sections.

Recently, Morpurgo and collaborators have theoretically studied the epimerization of 2-tetrahydropyranol catalyzed by organic compounds.[18,19] Their results also indicate a free aldehyde mechanism and a drastic reduction of the height of the barrier by solvent assistance. Furthermore, it has been shown that this catalyzed reaction is an asynchronous, concerted, double-proton transfer process, where one of the protons is transferred much earlier than the other.[18]

The aim of this paper is to present a quantum mechanical study of the mechanism of glucose mutarotation in the gas phase and in aqueous solution, considering the most abundant conformer of glucose, as well as a sophisticated continuum model to describe the bulk solvent effects. Additionally, we will also take into account the behavior of this reaction when the proposed mechanisms do or do not consider an explicit water solvent assistance in the gas phase and in aqueous solution.

Besides that we will try to estimate the rate coefficient of this process in aqueous solution using just theoretical calculations, in order to better compare the reaction pathways for the first time to the best of our knowledge.

2. Methodology and computational details

The pyranose and aldehyde forms of glucose used in this work are the α and β forms of the GT conformer, for which the dihedral angle ω = O5–C5–C6–O6 is approximately gauche (60°), as reported in Figure 2. These are the most abundant conformers found in aqueous solu-

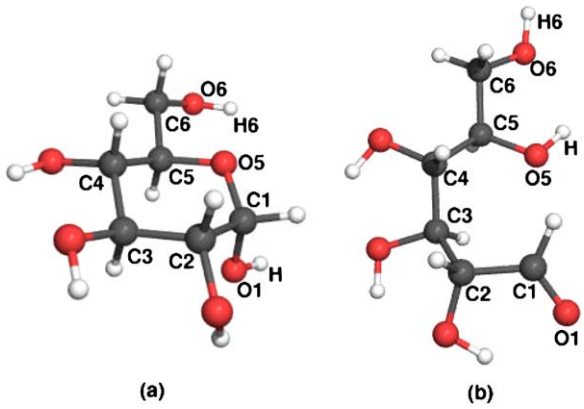

Figure 2. Pyranose (a) and aldehyde (b) forms of α-D-glucose. The atom labeling follows the standard adopted for carbohydrates.

tion, about 66% as reported in the literature (of which 44% in the α form and 56% β form).[17] The other α and β GG rotamers ($\omega = -60°$) are less abundant in aqueous solution (approximately 21%). However, as it cannot be considered as a negligible population, some considerations will also be outlined about their contribution to the mutarotation process, when properly mentioned.

The α and β conformers interconvert through an acyclic form, whose abundance in solution is negligible.

All the structures studied were determined at the B3LYP[20] level of calculation, using the 6-31+G(d,p) basis set. Considerations about the use of density functional calculations and this basis set are better presented in the work of Csonka,[21] who investigated the importance of diffuse functions when using density functionals to study carbohydrates. All the stationary points on the potential energy surface in the gas phase and in aqueous solution, corresponding to either a minimum or a transition structure, were characterized by the calculation of the respective vibrational frequencies. These calculations were performed using the Gaussian 03 program.[22] In this paper, we studied this reaction in the gas phase and in aqueous solution, following a protocol similar to that developed in recent work.[23,19] In order to define the role of the solvent in the mutarotation of glucose, we will consider basically four descriptions to this reaction, as indicated below.

Model 1: Gas phase. The mechanism is described only in the gas phase. The results obtained here come from the assumption that the proton transfer is only intramolecular, since there are no solvent molecules available.

Model 2: Continuum solvent. The system is studied in aqueous solution with a dielectric continuum description for the solvent. In this model we do not include any specific solute–solvent interaction. The proton transfer is also intramolecular, and the solvent does not take part in assisting it. There are just bulk electrostatic effects that collaborate to stabilize the reactants and transition structures.

Model 3: Microsolvation. The calculations are carried out in gas phase, but one water molecule is added to the structures of the stationary points of the reaction, in order to obtain a model for the stabilizing of hydrogen-bond interactions. In this case, the mechanism is considered to be water assisted by one solvent molecule. Bulk effects are not taken into account.

Model 4: Microsolvation and continuum. Models 2 and 3 are combined. The cluster consisting of glucose plus one water molecule is studied in a polarizable dielectric continuum media to make possible the analyses of both effects, the specific interactions coupled to the bulk effects.

Geometry optimization calculations were carried out to obtain the structures of reactants, products, and saddle points. After this, as already mentioned, their vibrational frequencies were obtained in order to check whether the stationary points were correctly located, that is, if there were just positive frequencies for reactants and products, and only one negative frequency for the transition state related to the bond that is broken. The intrinsic reaction coordinate has been followed in some cases to observe the evolution from the transition states to reactant and products, principally in the case of Model 4, where the potential energy surface is very shallow, with a large density of minima. The effects of solvation were determined using the integral equation formalism (IEF)[24] version of the polarized continuum solvation model (PCM).[25,26] In this approach the solute is represented as a quantum mechanical charge distribution inside a cavity of molecular shape immersed in a macroscopic dielectric with known permittivity ε. The electrostatic interaction between solute and solvent can then be represented in terms of a set of apparent surface charges located on the cavity. Such a cavity is built from interlocking spheres centered on atoms or group of atoms. The radii of these spheres are 1.80 Å for an O atom, 2.28 Å for the CH or CH_2 group of atoms, and 1.44 Å for H atoms of the hydroxyl groups. The solution of the resulting quantum mechanical problem gives the solute wave function modified by the solvent in a mutually polarized way. Within this approach, in the present study only the electrostatic component of the solvation energy was taken into account.

3. Results and discussion

3.1. Structures

Since the mechanism of glucose mutarotation that is not assisted by a water molecule is the same as that in the gas phase and in the continuum, the results of Models 1 and 2 will be discussed in parallel. The six corresponding

stationary points located on the potential energy surface of the system obtained from both models are reported in Figure 3. The structures reported were obtained from Model 1. A rigorous full treatment would also include an additional transition state between the α-open and β-open structures. However, since the corresponding barrier would surely be lower (it involves basically rotations about two bonds) than those between the pyranosidic forms and the respective transition states, this third transition structure was not considered in the mechanism.

The most important geometrical parameters are reported in Table 1. Initially, only the results in the gas phase will be considered, and afterwards those in the continuum.

Generally the most important changes are localized in the O1–H, O5–H, C1–O1, and C1–O5 bonds. The bond distances between the carbon atoms do not change significantly along these six structures.

In the first step of this reaction, the conversion of the α-pyranose to the α-open form through the four-centered saddle point α-TS, occurs via the intramolecular proton migration between the oxygen atoms O1 and O5, as evidenced by the changes of the O1–H from 0.967 Å in the α-pyranose to 1.315 Å in the α-TS. In the α-open form this proton is not bound more strongly to the oxygen atom O1.

The O5–H bond length (1.177 Å) in the α-TS changes to 0.969 Å in the α-open form, a very significant modification. Simultaneously with the proton migration of this first step, there is an opening of the pyranosidic ring and formation of the double bond C1–O1. The C1–O5 bond is stretched from 1.411 Å in the α-pyranose to 2.929 Å in the α-open structure. Simultaneously, the C1–O1 bond shows a shortening during the conversion of the α-pyranose to the α-open form from 1.419 to 1.218 Å, respectively, characterizing the formation of the aldehyde group C1HO1. The second step of this reaction, the con-

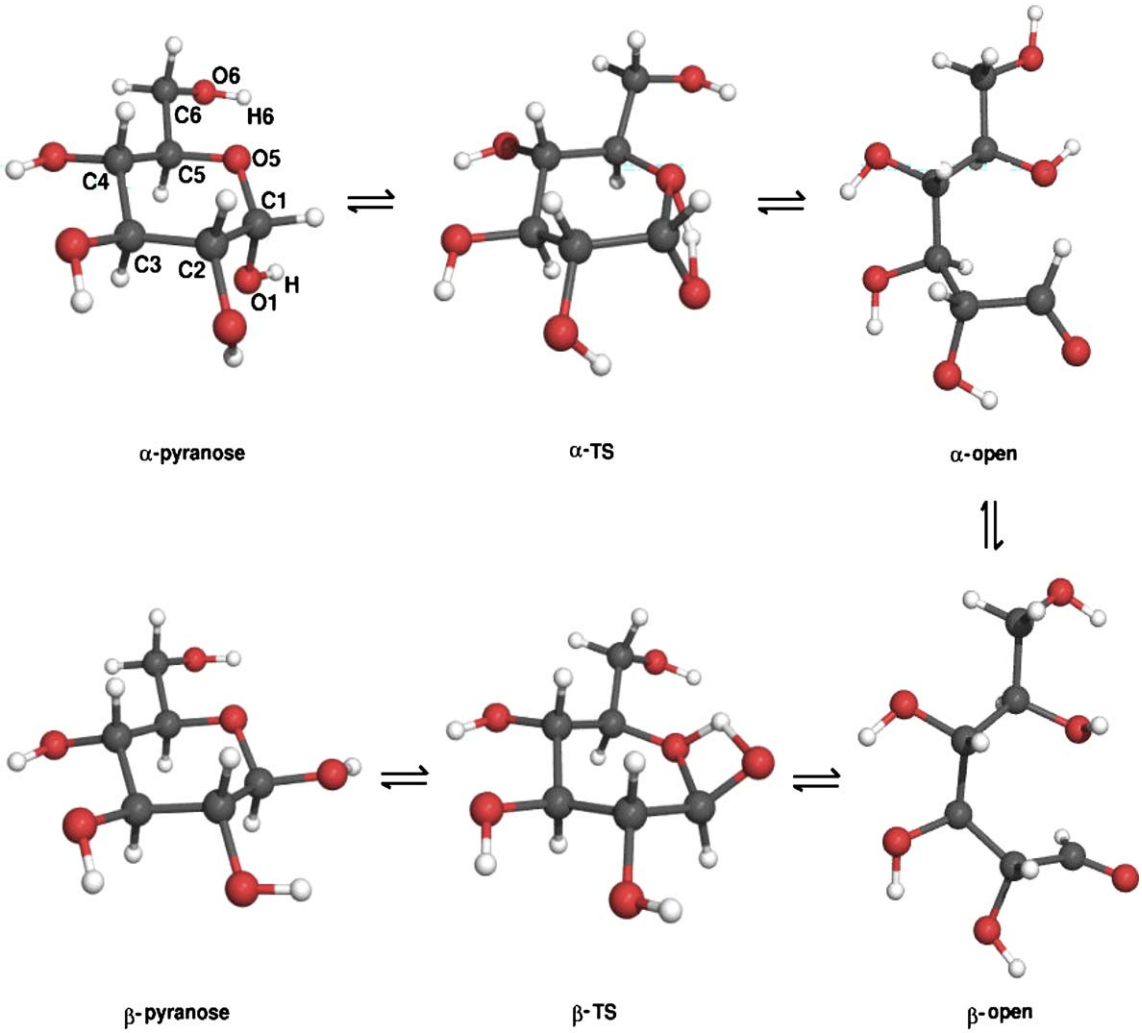

Figure 3. The concerted mechanism of mutarotation of D-glucose, obtained from Models 1 and 2, and their labels, used in the text. The reported structures are those obtained from Model 1.

Table 1. Geometric parameters for the stationary points of glucose mutarotation in the gas phase and in aqueous solution from Models 1 and 2[a]

Parameter	α-Pyranose		α-T		α-Open		β-Open		β-TS		β-Pyranose	
	(Å)	(°)	(Å)	(°)	(Å)	(°)	(Å)	(°)	(Å)	(°)	(Å)	(°)
Model 1												
C1–O1	1.419		1.323		1.218		1.214		1.311		1.397	
O5–C1	1.411		1.628		2.929		2.594		1.712		1.423	
O1–H	0.967		1.315			—		—	1.317		0.967	
O5–H		—	1.177		0.969		0.970		1.179			—
C1–O1–H		109.5		78.17		—		—		79.47		109.4
C5–O5–C1		111.4		126.8		—		—		127.9		113.4
C2–C1–O5–C5		−55.99		−2.385		—		—		−15.37		−62.98
C1–O5–C5–C4		58.95		11.950		—		—		21.74		62.1
C5–C6–O6–H6		−58.10		−62.15		−174.8		−46.24		−58.75		−57.63
Model 2												
C1–O1	1.414		1.341		1.221		1.220		1.333		1.397	
O5–C1	1.418		1.618		2.843		2.574		1.632		1.430	
O1–H	0.968		1.343			—		—	1.357		0.968	
O5–H		—	1.162		0.966		0.971		1.160			—
C1–O1–H		109.5		77.14		—		—		77.80		109.5
C5–O5–C1		115.7		127.8		—		—		127.8		113.3
C2–C1–O5–C5		−57.57		5.694		—		—		−19.88		−63.64
C1–O5–C5–C4		59.99		−1.610		—		—		24.66		63.1
C5–C6–O6–H6		−57.44		−66.51		−61.10		−53.02		−69.10		−57.91

[a] The labels refer to atoms as indicated in Figure 4. Bond distances are in Å, angles are in degrees (°).

version of the α-open form to the β-open form, does not drastically change the bond distances. This step is defined by rotations of the C1HO1 and O5–H groups around the C2–C1 and C5–O5 bonds, respectively. During these rotations, the C1–O5 bond is shortened from 2.929 Å in the α-open to 2.594 Å in the β-open form. The next and final step is the formation of a new pyranosidic ring, when the β-open form is converted to the β-pyranose form of glucose. This is exactly a reverse process of the first step discussed above. Then, the changes in the bond distances are similar to the ones in the first step, but in reverse order.

There are some changes in the angle values of these structures when the mutarotation is assumed to obey this mechanism. Similarly to the bond distance behavior, the angles between the carbon atoms do not show large variations along this reaction. The most important changes occur in the dihedral angle values. There can be observed large structural changes in these parameters during the conversion between the pyranoses and their corresponding open ring forms. This happens, for instance, for the C2–C1–O5–C5 and C1–O5–C5–C4 dihedral angles. In passing from the α-pyranose to the α-TS in the first step, the values change from −55.99° and 58.95° to −2.385° and 11.95°, respectively. These changes mean that the well-defined chair structure of the α-pyranose is vigorously distorted to another form in which these five atoms are almost in the same plane, defining almost an envelope structure for the saddle point. This ring deformation is evident and necessary to allow an intramolecular proton transfer.

The imaginary vibration frequencies (in cm^{-1}) of the α-TS and β-TS saddle points are −1621.5i and −1656.6i, respectively. The main components of the modes of these imaginary frequencies are, respectively, the O1–H and O5–H stretchings, as expected for these proton-migration reactions.

The behavior of this reaction described by Model 2, when just the bulk solvent effects are considered, is very similar to that found in Model 1. An analysis of the corresponding geometrical parameters (Table 1) reveals that the trend of the data of these two models is the same, with the exception of the dihedral angle C5–C6–O6–H in the α-open form. In Model 1 this dihedral angle is −174.8° and −61.10° in Model 2. That value for Model 2 allows an O5–H6 hydrogen bond that is not observed in Model 1, where the hydrogen bond occurs between the O6–H atoms. The respective hydrogen bond lengths are 2.487 and 2.220 Å.

In a general sense, the changes in the bond distances due to the mutarotation reaction are slightly more pronounced in the continuum medium (Model 2) than in the gas phase (Model 1).

Considering now Models 3 and 4, in light of the preceding discussion, the new important aspect to be introduced regards the participation of one solvent molecule in the proton-transfer reaction. It is not an intramolecular transfer any longer, but a concerted mechanism that follows a pseudo first-order reaction, if we consider the whole process to be an elementary reaction. In these models, one water molecule takes part in the proton transfer, leaving its proton and receiving another from the open glucose structure. This water molecule acts exactly as a catalyst, as we will see in the next section.

The structures obtained from such models are reported in Figure 4. Since they do not differ very much

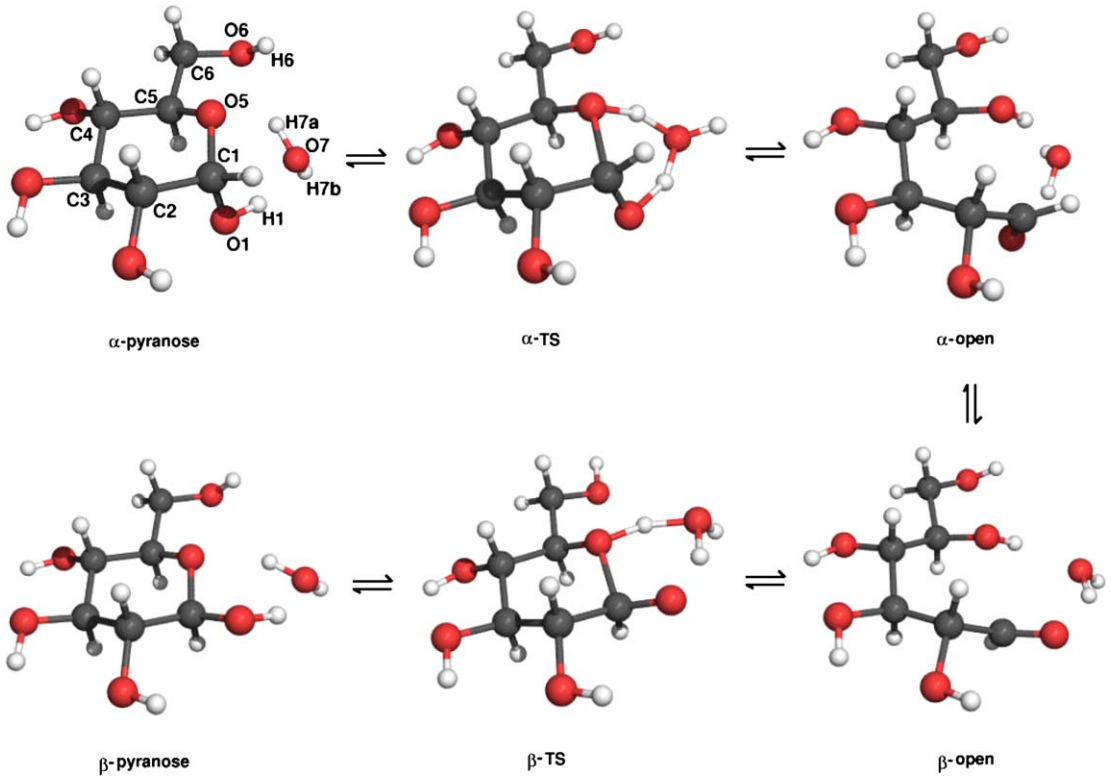

Figure 4. The concerted mechanism of glucose mutarotation, obtained from Models 3 and 4, and their labels used in the text.

from one model to the other, just those obtained from Model 3 will be presented. They are for the reaction that is assisted by one water molecule in the gas phase.

From data reported for Model 3, we can say that in the first step of this mechanism, the conversion of the α-pyranose to the α-open form through the six-centered saddle point α-TS, occurs via an intermolecular H7a proton migration from the oxygen atom O7 of the water molecule to the O5 atom. This is evidenced by the increases of the O7–H7a distance from 0.978 Å in the α-pyranose to 1.240 Å in the α-TS. In the α-open form this proton is not more strongly bonded to O7 of the water molecule. The O5–H7a bond length (2.894 Å) in the α-pyranose changes to 1.193 Å in the α-TS, and finally to 0.981 Å in the α-open form. Simultaneously, hydrogen atom H1 bonded to the O1 atom of glucose is transferred to the water molecule. This process can be accompanied by the changes in the distance values of the O1–H1 and H1–O7 bonds. This means, while the first is enlarged in the sequence of α-pyranose (0.980 Å), α-TS (1.266 Å) α-open (2.009 Å), the second is shortened for the same sequence of α-pyranose (1.912 Å), α-TS (1.172 Å) α-open (0.975 Å), which characterizes the proton transfer.

Simultaneously with the proton exchange of this first step, there is an opening of the pyranosidic ring and formation of the double bond C1–O1. The C1–O5 bond is stretched from 1.430 Å in the α-pyranose to 2.562 Å in the α-open structure. In parallel, the C1–O1 bond shows a shortening during the conversion of the α-pyranose to α-open form, from 1.393 to 1.219 Å, respectively, which characterizes the formation of the aldehyde group C1HO1. As happened in Models 1 and 2, the second step of this reaction, the conversion of the α-open form to the β-open form, does not drastically change in the bond distances. This step is governed by rotations of the C1HO1 and O5–H7a groups around the C2–C1 and C5–O5 bonds, respectively, the first being much more pronounced than the second. During these rotations, the C1–O5 bond is shortened from 2.562 Å in the α-open form to 2.476 Å in the β-open form, a shortening that is less pronounced than that observed in Models 1 and 2. The next and final step is the formation of a new pyranosidic ring, when the β-open form is converted to the β-pyranose form of glucose. This is exactly the reverse process of the first step discussed above. Then, the changes in the bond distances are similar to the ones in the first step, but, again, in reverse order.

There are not any important changes in the angle values of these structures when the mutarotation is assumed to obey this mechanism. The six-membered ring formed by the water molecule and the –H1–O1–C1–O5– moiety reduces very much the tension among the atoms, and the chair conformation is maintained during the whole process of interconversion between the alpha and beta structures. It is also observed that the $-CH_2OH$

group of the monosaccharide helps maintain the proper orientation of the water molecule.

The imaginary vibration frequencies (in cm^{-1}) of the α-TS and β-TS saddle points are −1406.00i and −1107.52i, respectively. The main components of the modes of these imaginary frequencies are, respectively, the O1–H1–H and O5–H7a–O7 stretchings, as expected for these proton-migration reactions.

The behavior of this reaction described by Model 4, when the bulk effects are considered, is very similar to that found in Model 3. An analysis of the corresponding geometrical parameters (Table 2) reveals that the trends of the data of these two models are basically the same.

3.2. Thermodynamics and kinetics

In this section the thermodynamic and kinetic aspects of the two mechanisms studied are analyzed following the results obtained from each of the four models.

Figures 5 and 6 show the free-energy profiles of the reactions for Models 1 and 2, respectively. In order to obtain the free-energy ($G^0_{298\,K}$) values for the structures considered, thermal and entropic corrections were taken into account for each stationary point of the potential energy surfaces.

Considering the results obtained from Model 1, since the α-pyranose structure is the most stable one, its energy value will be used as the reference value in the following. The height of the highest barrier expressed as $\Delta G^{\ddagger}_{298\,K}$ is 41.79 kcal/mol for the α-pyranose→α-open form conversion, and 43.09 kcal/mol for β-pyranose→β-open form. They are considerably higher than the experimental values of approximately 22 kcal/mol.[12] This high theoretical barrier can be explained in terms of the enormous tension imposed on the pyranosidic ring of the saddle point structures during their flattening. It can also be seen that the α-open form is more stable than the β-open form by 4.86 kcal/mol, and the α-pyranose is more stable than the β-pyranose as well. These findings are in perfect agreement with the manifestation of the anomeric effect.[27]

On the other hand, when the results obtained from Model 2 are considered, the first important difference is related to the larger stability of the β-pyranose form when compared to the α-pyranose. In fact, this structure is now considered as the reference structure.

Table 2. Geometric parameters for the stationary points of mutarotation of glucose in the gas phase and in aqueous solution for Models 3 and 4[a]

Parameter	α-Pyranose		α-TS		α-Open		β-Open		β-TS		β-Pyranose	
	(Å)	(°)	(Å)	(°)	(Å)	(°)	(Å)	(°)	(Å)	(°)	(Å)	(°)
Model 3												
C1–O1	1.393		1.291		1.219		1.221		1.296		1.385	
O1–H1	0.980		1.266		2.009		2.036		1.397		0.976	
O5–C1	1.430		1.763		2.562		2.476		1.680		1.438	
O5–H7a	2.894		1.193		0.981		0.977		1.198		2.128	
O7–H7a	0.978		1.240		1.827		1.887		1.231		0.973	
O7–H7b	0.964		0.965		0.965		0.964		0.966		0.965	
O7–H1	1.912		1.172		0.975		0.974		1.091		1.970	
C1–O1–H1		108.7		103.0		—		—		104.5		107.84
C5–O5–C1		113.7		116.1		—		—		114.2		113.32
O5–H7a–O7		98.64		157.9		—		—		151.8		130.75
H7a–O7–H7b		107.0		117.9		—		—		114.1		107.20
H7a–O7–H1		109.2		87.88		98.80		107.8		89.8		93.61
C2–C1–O5–C5		−63.13		−54.2		—		—		−76.66		−63.78
C1–O5–C5–C4		65.65		53.32		—		—		65.63		61.91
C5–C6–O6–H		−72.31		−68.93		−68.86		−74.16		−176.10		−83.89
Model 4												
C1–O1	1.403		1.300		1.223		1.222		1.311		1.393	
O1–H1	0.984		1.400		2.080		2.157		1.424		0.981	
O5–C1	1.426		1.720		2.587		2.531		1.645		1.429	
O5–H7a	2.715		1.176		0.983		0.981		1.204		2.263	
O7–H7a	0.980		1.261		1.810		1.845		1.227		0.976	
O7–H7b	0.967		0.969		0.967		0.967		0.970		0.967	
O7–H1	1.862		1.079		0.974		0.973		1.080		1.940	
C1–O1–H1		107.05		101.28		—		—		103.02		106.30
C5–O5–C1		114.26		115.95		—		—		114.90		113.01
O5–H7a–O7		103.09		157.56		—		—		152.99		119.44
H7a–O7–H7b		105.90		113.50		—		—		114.15		106.27
H7a–O7–H1		104.00		88.70		106.09		106.03		88.69		99.26
C2–C1–O5–C5		−62.21		−55.63		—		—		−65.50		−66.95
C1–O5–C5–C4		65.48		54.58		—		—		63.76		66.69
C5–C6–O6–H		−168.14		−79.85		−67.45		−74.63		−104.10		−177.06

[a] The labels refer to atoms as indicated in Figure 4. Bond distances are in Å, angles are in degrees (°).

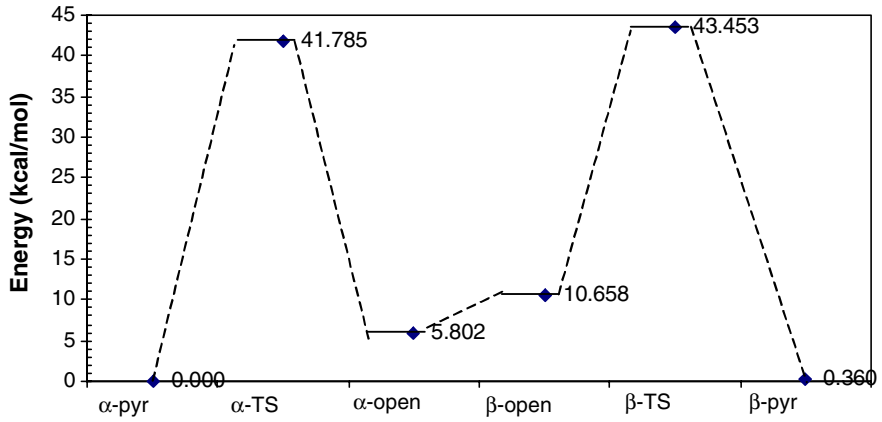

Figure 5. The Gibbs free-energy profile for the reaction in Model 1, in kcal/mol. $G_{298\ K}$ (α-pyranose = −687.072922 a.u.).

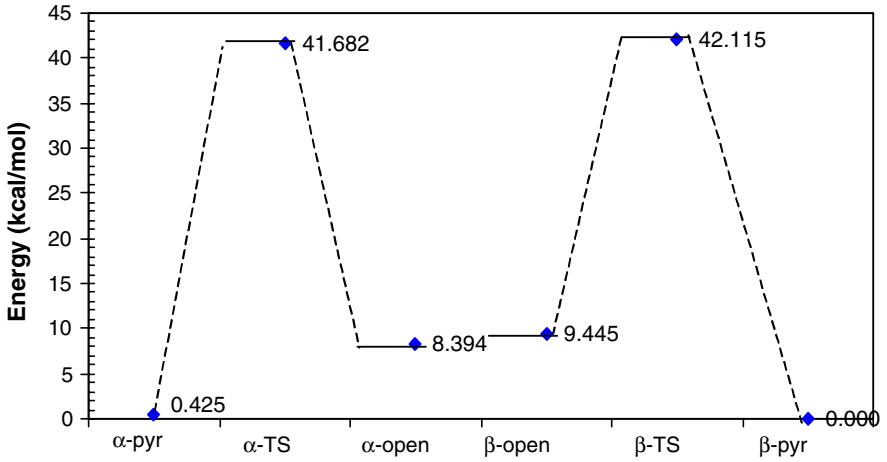

Figure 6. The Gibbs free-energy profile for the reaction in Model 2, in kcal/mol. $G_{298\ K}$ (β-pyranose = −687.098830 a.u.).

The interaction with a high-dielectric solvent brings more stability to the β-form, since it has a higher dipole moment than the α-form. Therefore, since we can see that a dielectric continuum model is able to properly describe the thermodynamics of the system, it means that there is a relative abundance of the β pyranosidic structure over that of the α conformer.[28] However, the general consequence of the bulk, considered as a polarizable dielectric continuum, seems to be the lowering of the height of the barriers for the mutarotation process by approximately 1 kcal/mol, a value that is below the accuracy of the theoretical description employed and far from the lowering needed to bring the barrier height close to the observed value.

It can be said that the open structures are more sensitive to the solvent presence than the cyclic structures. While the β-open form is stabilized when the system passes from the gas phase (Model 1) to solution (Model 2) by 1 kcal/mol, the α-open structure is destabilized by approximately 2.5 kcal/mol. Due to solvent presence, the open structures interconvert more easily. However, the solvent continuum by itself is insufficient to correctly describe the whole reaction, since our theoretical models furnish results that are still very different from the experimental ones.

The energy profiles of the mechanisms described in Models 3 and 4 are shown in Figures 7 and 8. A drastic difference can be observed between the two, although the β-pyranose form remains the reference structure in both cases.

In Model 3 the barriers between the pyranosidic and open structures are lowered substantially by the assistance of the water molecule. The set of β structures is more stable than the corresponding α structures. The barrier between α-pyranose and α-TS is now just 27.9 kcal/mol, while that between the β-pyranose and β-TS forms is 24.8 kcal/mol. These barriers are approximately 13 kcal/mol lower than those obtained from Models 1 and 2. Such findings are surely related to the maintenance of the chair conformation when the mechanism is assumed to evolve with solvent assistance.

Passing finally to Model 4, it can be said that the pattern observed for Model 3 is repeated. The set of β structures is kept more stable than the α ones. The

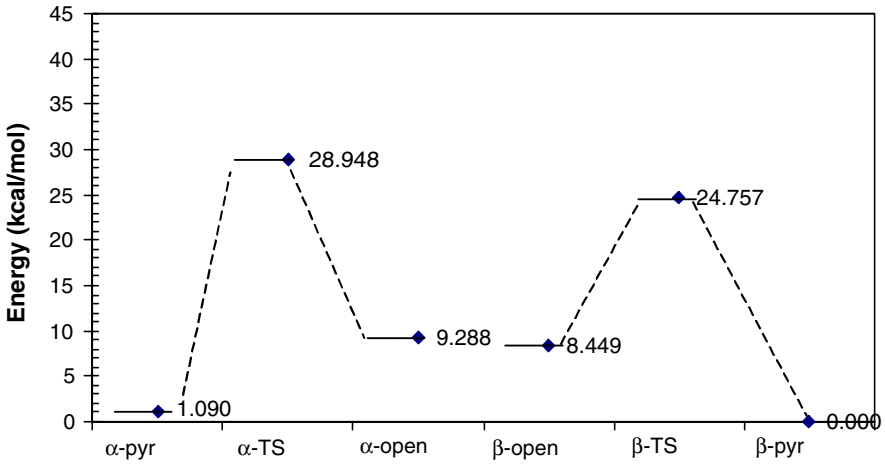

Figure 7. The Gibbs free-energy profile for the reaction in Model 3, in kcal/mol. $G_{298\ K}$ (β-pyranose = −763.498646 a.u.).

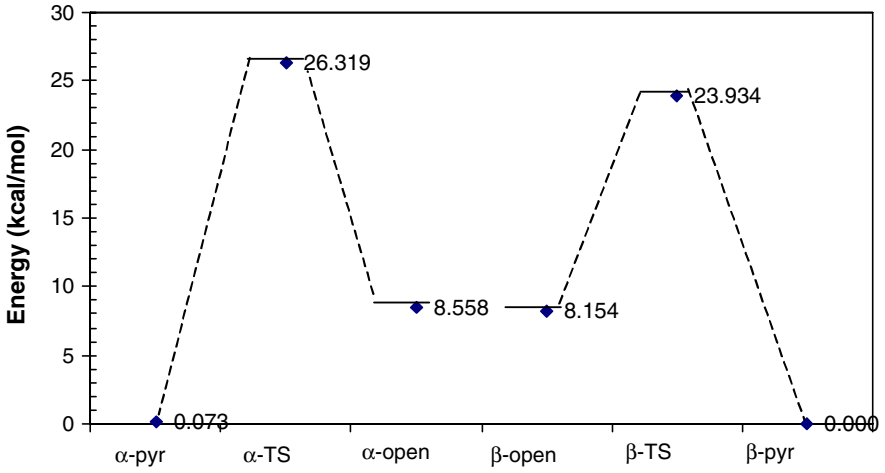

Figure 8. The Gibbs free-energy profile for the reaction in Model 4, in kcal/mol. $G_{298\ K}$ (β-pyranose = −763.526751 a.u.).

interconversion barriers between both the α and β pyranoses and each respective TS became 26.2 and 23.9 kcal/mol, respectively, for the GT rotamer. The effect of the solvent, considered as a dielectric continuum, is very smooth; it acts basically by facilitating the whole process. Only this model was applied to the GG rotamer, and although less abundant than the GT structure, the mutarotation process is favored in the former. The height of the barriers are 23.7 kcal/mol for the α-pyranose→α-TS transition and 23.1 kcal/mol for the β-pyranose→β-TS transition. Adopting here the effective free-energy concept,[23] which applies the Arrhenius formula assuming that the rate constants of the individual channels can be summed to give the total rate constant, the new values for the barriers are 23.68 kcal/mol for the α-pyranose→α-TS transition and 22.92 kcal/mol for the β-pyranose→β-TS transition, considering both GT and GG conformers.

There is much controversy in the literature in regard to the number of water molecules involved in mutarotation. Theoretical[15] and experimental[12] works discuss the possibility of two or three water molecules taking part in the mechanism. However, considering some previous theoretical results, and some findings obtained from our work, some explanations can be outlined.

The energy profiles for the glucose mutarotation reported by Yamabe and Ishikawa,[15] assisted by *n* water molecules (*n* = 0, 1, 2, and 3) were built taking as the reference value not the corresponding α-pyranose or β-pyranose structure. Therefore, we have decided, in order to make better comparisons, to rescale all the barriers found for these authors, taking as the reference energy value that which was obtained for the corresponding α-pyranose *n* solvated structure. Doing so, the values in Table 3 can be obtained.

From the values in Table 3, it can be seen that the first water molecule lowers the mutarotation barrier by 20.02 kcal/mol for the α structure and 18.21 kcal/mol for the β structure. The second water molecule, instead, has much less intense effect on the height of the barrier.

Table 3. Height of the energy barriers for the mutarotation of glucose assisted by *n* water molecules, following the work of Yamabe and Ishikawa[15]

n	Energy[a]				
	α-Pyranose	α-TS	Open	β-TS	β-Pyranose
0	0	50.84	12.00	49.19	2.07
1	0	30.82	11.80	29.17	0.26
2	0	29.23	10.70	27.49	1.16
3	0	24.88	—	—	—

[a] In kcal/mol.

The barrier between the α-pyranose and α-TS structures is lowered just by 1.59 kcal/mol, while the barrier between β-TS and β-pyranose diminishes by 2.58 kcal/mol. If a third water molecule is considered, a new lowering of 4.35 kcal/mol is obtained for the α-pyranose→α-TS barrier. It is important to notice that the β-pyranose structures are not obtained as more stable entities than the α-pyranose conformers, and this can raise some doubts about the proper description of the conformations found for the pyranosidic structures. Even neglecting these small inconsistencies, it is clear from the results of Yamabe and Ishikawa that the second water molecule plays a role very different from the first one, which, in fact, changes the mutarotation mechanism. The third water molecule would again have a catalytic effect, since it lowers the proton-transfer activation energy by 4–5 kcal/mol. However, from the chemical point of view, such a situation is quite improbable, principally if it is taken into account that such structures were not obtained from any dynamic simulation, and so the resident time of the clusters obtained are not known.

In fact, some calculations at the B3LYP/6-31+G(d,p) level were performed taking the geometries of Yamabe and Ishikawa as the starting geometries, consisting of two and three water molecules only for Models 3 and 4. The results are collected in Table 4.

The numbers in Table 4 show that a dielectric continuum polarizable medium as described by PCM furnishes a very distinctive description from that offered by the Onsager model. Two or three water molecules have approximately the same effect on the mutarotation of glucose. However, both pathways have a height of the barrier for the mutarotation lower than the experimental value, and so, maybe can be only a mathematical solution, not having any physical relevance. It is important to stress that only a dynamic study involving at least the α-pyranose structure can bring more light to this discussion.

Table 4. $\Delta G^0_{298\,K}$ values for the height of the α-pyranose→α-TS barrier in kcal/mol

$\Delta G^0_{298\,K}$[a]	$n = 2$	$n = 3$
Model 3	21.84	21.57
Model 4	20.93	21.32

[a] In kcal/mol.

3.3. Rate coefficients

In order to check the mechanisms studied, the rate coefficients of each step of the mutarotation were theoretically obtained using transition-state reaction-rate theory (TST).[29] It is based on the application of statistical mechanics to reactants and the corresponding activated complex (TS). The rate coefficient (k) for the mutarotation of glucose is given by Eq. 1

$$k = \frac{k_B T}{h} N_A \frac{Q^{\neq}}{Q_A} e^{-(\Delta E^{\neq}_{act})/RT} \quad (1)$$

where h, N_A, k_B, and R are Planck, Avogadro, Boltzmann, and ideal gas constants, respectively. T is the temperature of the system, E_{act} is the activation barrier, which already includes the zero-point energy correction. In the equation, $Q^{\neq}$ and Q_A are the partition functions for the transition state and for the reactant A, respectively. Each partition function is written as the product $Q = q_{rot} \cdot q_{vib} \cdot q_{eletr} \cdot q_{trans}$, where the first two components q_{rot} and q_{vib} are the rotational and vibrational partition functions, obtained from the second derivatives of the energy regarding the nuclear coordinates. Since only one electronic state is considered, $q_{eletr} = 1$, and q_{trans} is assumed to be similar for both reactants and the transition structures, it was thus cancelled out in Eq. 1.

In the gas phase, this approach is immediate once the second derivatives for each stationary point corresponding to each structure involved in the mechanism is calculated. However, in aqueous solution, to the best of our knowledge, this is the first time that it has been tested, assuming a dielectric continuum description for the solvent. In this case, the tacit assumptions are: (1) The partition function in solution can be factorized and written as a product of the partition function for the solute (glucose in the case of Model 1, and glucose plus 1 water molecule in the case of Model 2) and the partition function of the solvent. (2) The partition function for the solvent is approximately the same in the case of the transition structure and in the case of the reactant. Thus both terms cancel out in the expression, leaving just the Q for the solute (TS and reactant), which is directly obtained from the second derivatives of the PCM model. In this case the $\Delta E^{\neq}_{act}$ is replaced by the corresponding quantity in solution, which is the Gibbs free energy of the solute in aqueous solution, corrected just by the zero-point energy.[30] The values obtained for the coefficient rates within the limits of this approach are reported in Table 5.

From data reported in Table 5, it can be seen that Model 4 gives the rate coefficients closest to the experimental values. The values found for k_α and k_β are in

Table 5. Rate coefficients (k) for the glucose mutarotation, in seg^{-1}, assuming the reaction obeys pseudo first-order kinetics

	k_α	k_β
Model 1	1.4741×10^{-18}	1.6566×10^{-19}
Model 2	3.6043×10^{-18}	8.5036×10^{-19}
Model 3	2.4355×10^{-8}	4.6051×10^{-6}
Model 4 (GT)	3.6091×10^{-7}	1.7845×10^{-5}
Model 4 (GG)	6.6612×10^{-5}	7.6988×10^{-5}
Model 4 (GG+GT)	6.6473×10^{-5}	9.4833×10^{-5}
Exp.[31]	3.5167×10^{-4}	2.3389×10^{-4}
Exp.[12a]	2.3233×10^{-4}	1.3667×10^{-4}
Exp.[12b]	4.0546×10^{-4}	2.412×10^{-4}

very good agreement with the experimental values when the effective free-energy concept is adopted (disregarding the rotamer interconversion during the mutarotation), which corresponds to the Model 4 (GT+GG) values. At any rate, the search for a full numerical agreement can be misleading in this case, where the accuracy of the theoretical calculation (approximately 1 kcal/mol) is exponentially related to the rate coefficient. Besides that, it is important to notice that only two glucose conformers were considered. Other structures are also present in solution, which were not considered in this work, contributing to the existence of other reaction pathways and consequently to the increase of k.

4. Conclusions

In this work the glucose mutarotation mechanism is investigated theoretically. Two machanisms are studied. One assumes the process is intramolecular, and the other assumes it is solvent-assisted by one water molecule. The most stable α and β GT conformers in aqueous solution were considered, and a B3LYP/6-31+G(d,p) description was adopted for the system. Four theoretical models were used in order to also evaluate the role of the other water molecules in the whole process.

The results obtained have shown that mutarotation is a solvent-assisted process that obeys pseudo first-order kinetics. Besides that, the first water molecule from the solvent acts as a catalyst, and plays a decisive role, since it completely changes the mutarotation mechanism. The other solvent molecules, in contrast to proposals in other work,[15] were shown here to basically exert a bulk solvent effect that was successfully described by a continuum polarazible model.

The rate coefficients for the glucose mutarotation reaction, theoretically obtained for the first time in aqueous solution, to the best of our knowledge, were calculated for our different approaches. Their agreement with the experimental values is an important indication that the mechanism most favored is the one that is solvent assisted by only one solvent molecule.

Acknowledgments

C. O. da Silva thanks the Brazilian agencies CNPq, CAPES, and FAPERJ for financial support given to this work.

References

1. Voet, D.; Voet, J. G. *Biochemistry*; John Wiley & Sons: New York, 1995.
2. Capon, B. *Chem. Rev.* **1969**, *69*, 407–498.
3. Rao, V. S. R.; Qasba, P. K.; Baslaji, P. V.; Chandrasekaran, R. *Conformation of Carbohydrates*; Harwood Academic: Amsterdam, 1998.
4. Brønsted, J. N.; Guggenheim, E. A. *J. Am. Chem. Soc.* **1927**, *49*, 2554–2584.
5. Lowry, T. M. *J. Chem. Soc.* **1927**, *129*, 2554–2565.
6. Swain, C. G.; Di Milo, A. J.; Cordner, J. P. *J. Am. Chem. Soc.* **1958**, *80*, 5983–5988.
7. Pedersen, K. J. *J. Phys. Chem.* **1934**, *38*, 581–600.
8. Swain, C. G. *J. Am. Chem. Soc.* **1950**, *72*, 4578–4583.
9. (a) Cantor, S. M.; Peniston, Q. P. *J. Am. Chem. Soc.* **1940**, *62*, 2113–2121; (b) Wiesner, K. *Collect. Czech. Chem. Commun.* **1947**, *12*, 64–68; (c) Los, J. M.; Simpson, L. B.; Wiesner, K. *J. Am. Chem. Soc.* **1956**, *78*, 1564–1568.
10. Eigen, M. *Discuss. Faraday Soc.* **1965**, *39*, 7–15.
11. (a) Huang, H. H.; Robinson, R. R.; Long, F. A. *J. Am. Chem. Soc.* **1966**, *88*, 1866–1872; (b) Huang, H. H.; Yeo, A. N. H.; Chia, L. H. L. *J. Chem Soc. B* **1969**, 836–840.
12. (a) Ballash, N. M.; Robertson, E. B. *Can. J. Chem.* **1973**, *51*, 556–560; (b) Gram, F.; Hveding, J. A.; Reine, A. *Acta Chem. Scand.* **1973**, *27*, 3616–3619; (c) Livingstone, G.; Franks, F.; Aspinall, L. J. *J. Solution Chem.* **1977**, *6*, 203–216.
13. Capon, B.; Walker, R. *J. Chem. Soc., Perkin Trans. 2* **1974**, 1600–1610.
14. Rittenberg, D.; Graff, C. *J. Am. Chem. Soc.* **1956**, *80*, 3370–3372.
15. Yamabe, S.; Ishikawa, T. *J. Org. Chem.* **1999**, *64*, 4519–4524.
16. Onsager, L. *J. Am. Chem. Soc.* **1938**, *58*, 1486–1493.
17. (a) Barrows, S. E.; Storer, J. W.; Cramer, J. C.; French, A. D.; Truhlar, D. G. *J. Comput. Chem.* **1998**, *19*, 1111–1129; (b) Cramer, C. J.; Truhlar, D. G.; French, A. D. *Carbohydr. Res.* **1997**, *298*, 1–14; (c) Cramer, C.; Truhlar, D. G. *J. Am. Chem. Soc.* **1993**, *115*, 5745–5753; (d) Silva, C. O.; Mennucci, B.; Vreven, T. *J. Org. Chem.* **2004**, *69*, 8161–8164.
18. Morpurgo, S.; Brahimi, M.; Bossa, M.; Morpurgo, G. O. *Phys. Chem. Chem. Phys.* **2000**, *12*, 2707–2713.
19. Morpurgo, S.; Bossa, M. *Phys. Chem. Chem. Phys.* **2003**, *5*, 1181–1189.
20. (a) Lee, C.; Yang, W.; Parr, R. G. *Phys. Rev. B* **1988**, *37*, 785–792; (b) Becke, A. D. *J. Chem. Phys.* **1993**, *98*, 5648–5652.
21. Csonka, G. *J. Mol. Struct. (THEOCHEM)* **2002**, *584*, 1–4.
22. Frisch, M. J.; Trucks, G. W.; Schlegel, H. B.; Scuseria, G. E.; Robb, M. A.; Cheeseman, J. R.; Montgomery, J. A., Jr.; Vreven, T.; Kudin, K. N.; Burant, J. C.; Millam, J. M.; Iyengar, S. S.; Tomasi, J.; Barone, V.; Mennucci, B.; Cossi, M.; Scalmani, G.; Rega, N.; Petersson, G. A.; Nakatsuji, H.; Hada, M.; Ehara, M.; Toyota, K.; Fukuda, R.; Hasegawa, J.; Ishida, M.; Nakajima, T.; Honda, Y.;

Kitao, O.; Nakai, H.; Klene, M.; Li, X.; Knox, J. E.; Hratchian, H. P.; Cross, J. B.; Adamo, C.; Jaramillo, J.; Gomperts, R.; Stratmann, R. E.; Yazyev, O.; Austin, A. J.; Cammi, R.; Pomelli, C.; Ochterski, J. W.; Ayala, P. Y.; Morokuma, K.; Voth, G. A.; Salvador, P.; Dannenberg, J. J.; Zakrzewski, V. G.; Dapprich, S.; Daniels, A. D.; Strain, M. C.; Farkas, O.; Malick, D. K.; Rabuck, A. D.; Raghavachari, K.; Foresman, J. B.; Ortiz, J. V.; Cui, Q.; Baboul, A. G.; Clifford, S.; Cioslowski, J.; Stefanov, B. B.; Liu, G.; Liashenko, A.; Piskorz, P.; Komaromi, I.; Martin, R. L.; Fox, D. J.; Keith, T.; Al-Laham, M. A.; Peng, C. Y.; Nanayakkara, A.; Challacombe, M.; Gill, P. M. W.; Johnson, B.; Chen, W.; Wong, M. W.; Gonzalez, C.; Pople, J. A. *Gaussian 03, Revision B.01*; Gaussian: Pittsburgh, 2003.

23. da Silva, C. O.; Mennucci, B.; Vreven, T. *J. Phys. Chem. A* **2003**, *107*, 6630–6637.
24. Cancès, E.; Mennucci, B.; Tomasi, J. *J. Chem . Phys.* **1997**, *107*, 3032–3038.
25. Miertus, S.; Scrocco, E.; Tomasi, J. *Chem. Phys.* **1981**, *55*, 117–129.
26. Cammi, R.; Tomasi, J. *J. Comput. Chem.* **1995**, *16*, 1449–1458.
27. Tvaroška, I.; Bleha, T. *Adv. Carbohydr. Chem. Biochem.* **1989**, *47*, 45–123.
28. da Silva, C. O.; Mennucci, B.; Vreven, T. *J. Org. Chem.* **2004**, *69*, 8161–8164.
29. (a) Gilbert, R. G.; Smith, S. C. *Theory of Unimolecular and Recombination Reactions*; Blackwell: Oxford, UK, 1990; (b) Steinfeld, J. I.; Francisco, J. S.; Hase, W. L. *Chemical Kinetics and Dynamics*; Prentice-Hall: New York, 1989.
30. Tomasi, J. *Theor. Chem. Acc.* **2004**, *112*, 184–189.
31. Le Barc'H, N.; Grossel, J. M.; Looten, P.; Mathlouthi, M. *Food Chem.* **2001**, *74*, 119–122.